논문 2004-41TC-12-12

개구면 결합 공진기 급전 마이크로스트립 패치 안테나의 회로망 해석 및 설계

(Network Analysis and Design of Aperture-Coupled Cavity-Fed Microstrip Patch Antenna)

신 종 우*, 김 정 필**

(Jong Woo Shin and Jeong Phill Kim)

요 약

본 논문은 개구면 결합 공진기 급전 마이크로스트립 패치 안테나에 대하여 간결하면서도 정확한 등가회로 모델을 추출하기 위한 일반적인 전자기 이론을 제안하였다. 그리고 등가회로는 이상적인 트랜스, 어드미턴스, 그리고 전송선으로 구성된다. 관련 소자들의 값은 복소전력 개념, Fourier 변환, Fourier 급수, 그리고 spectral-domain immittance-approach를 적용하여 계산된다. 본 논문에서는 이 방법을 이용하여 안테나의 입력 임피던스를 구하고, 기존 논문에서 발표된 계산값, 그리고 측정값들과 비교하였다. 기존의 연구 결과와의 정확한 일치는 본 논문이 제안한 등가회로 모델의 간결성과 정확성을 입증해 준다.

Abstract

This paper presents a general theory for the analysis of an aperture-coupled cavity-fed microstrip patch antenna to develop a simple but accurate equivalent circuit model. The developed equivalent circuit consists of ideal transformers, admittance elements, and transmission lines. These circuit element values are computed by applying the complex power concept, the Fourier transform and series representation, and the spectral-domain immittance approach. The input impedance of the antenna is calculated and compared with the published data. Good agreements validate the simplicity and accuracy of the developed equivalent circuit model.

Keywords: microstrip patch antenna, aperture-coupled, cavity-fed, network analysis, CAD.

I. INTRODUCTION

An aperture-coupled feed has been proposed to improve the characteristics of a microstrip patch antenna[1], where the performance of the patch and the feed circuitry can be optimized independently by choosing the thickness and dielectric constant of the corresponding substrates. Recently, a thick ground plane was added to the aperture-coupled microstrip patch antenna to serve as a heat sink for active monolithic microwave integrated circuits (MMIC) and to provide structural support for thin substrates[2][3]. The coupling aperture through the thick ground plane of this antenna has a uniform cross section and behaves as a waveguide below the cutoff frequency. Consequently, the level of coupling from the feed line to the patch decays rapidly with increasing ground-plane thickness[4]. The coupling level can be restored by increasing the aperture length, but this in turn increases unwanted back radiation.

For applications requiring an electrically thicker

* 학생회원, ** 정회원, 중앙대학교
(School of Eletrical and Eletronic Engineering Chung-Ang University)

※ 이 논문은 2003학년도 중앙대학교 학술연구비 지원에 의한 것임.

접수일자: 2004년7월29일, 수정완료일: 2004년11월16일

ground plane, the aperture-coupled cavity-fed microstrip patch antenna was proposed by replacing the aperture of uniform cross section with a cavity and two coupling apertures with independent sizes[5]. The cavity in this antenna, which operates above the cutoff frequency, can provide good coupling efficiency through a ground plane of any thickness while maintaining a small aperture in the feed side to minimize back radiation. In addition, the cavity-fed patch has additional degrees of design freedom compared with the patch with a uniform aperture and so can, potentially, be optimized for improved antenna performance.

The numerical method of moments has been used to determine the antenna impedance[5]. But this approach needs too much computation time, and is lack of providing us a physical understanding of operating mechanism as well as some initial design data of the antenna. In this paper, a general method of analysis for aperture-coupled cavity-fed microstrip patch antennas is proposed with a view to developing an accurate equivalent circuit model for efficient computer-aided design of the antenna.

II. ANALYSIS METHOD

Fig. 1 shows a structure of an aperture-coupled cavity-fed microstrip patch antenna. A rectangular microstrip patch antenna is located on the top plane of the upper substrate with a dielectric constant ϵ_{rp} and a thickness h_p. W_p and L_p are the width and the length of the antenna. A microstrip feed line is placed on the bottom plane of the lower substrate with a dielectric constant ϵ_{rf} and a thickness h_f. W_f is a width of feed line and L_f is the stub length of microstrip feed line. Aperture 1 with a width W_{a1} and a length L_{a1} is located on the ground plane of the feed line, and aperture 2 with a width W_{a2} and a length of L_{a2} is placed on the ground plane of the patch antenna; a, b and t are the width, height, and length of a rectangular waveguide cavity. ϵ_{rw} is the

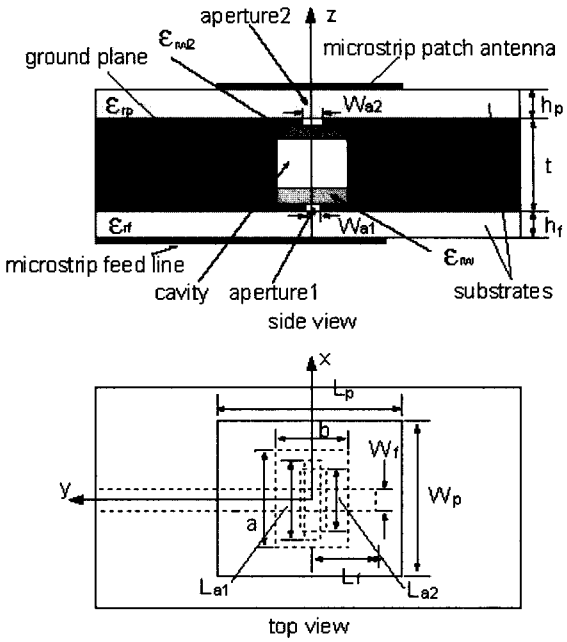

그림 1. 개구면 결합 공진기 급전 마이크로스트립 패치 안테나의 구조

Fig. 1. Geometry of an aperture-coupled cavity-fed microstrip patch antenna.

dielectric constant of the dielectric material in the waveguide cavity.

For the time being, consider an aperture-coupled microstrip patch antenna with a zero thickness ground plane. If the patch is treated as a microstrip line, the antenna can be viewed as aperture-coupled back-to-back microstrip lines[6]. Its equivalent network model was developed[7] where the existence of stored energy near the aperture was modeled by a slotline terminated by an extended short circuit. However, the effects of aperture radiation and a thick ground plane are not taken into account in this case. Therefore to accommodate these effects accurately, the equivalent circuit model mentioned above must be modified.

In this paper, the effect of the complex power flow into the lower half space from aperture 1 is represented by admittance Y_f. Similarly, another admittance Y_p is introduced to represent the effect of the complex power flow into the upper half space from aperture 2. If a cavity with two apertures is modeled successfully, the antenna can be represented by the equivalent circuit shown in Fig. 2, where Z_{0f}

and β_f, Z_{0p} and β_p are the characteristic impedances and phase constants of the microstrip feed line and the microstripline model of the patch, respectively. G_r is the radiation conductance at the end of the patch, and ΔL_p and ΔL_f are the extended microstripline lengths due to the non-zero inductance at the end[8].

1. Evaluation of Turns Ratios

It is well known that coupling between the microstripline and aperture in the ground plane can be modeled by an ideal transformer as shown in the equivalent circuit Fig. 2. For ΔV_f and V_f, the microstripline voltage discontinuity due to the aperture on the ground plane and the aperture voltage, respectively, the turns ratio of the ideal transformer $n_f(=\Delta V_f/V_{af})$ can be expressed by invoking the reciprocity theorem[9][10] as

$$n_f = \iint_{S_a} (\bar{e}_a \times \bar{h}_f) \cdot \hat{n}\, dS, \tag{1}$$

where S_a is the aperture area, $\bar{e}_a$ is the aperture electric field, $\bar{h}_f$ denotes the magnetic field of a microstrip feed line under the normalization condition of unit current flow, and $\hat{n}$ is the outward normal unit vector. With the following assumed aperture electric field $\bar{e}_a = \hat{y} e_y$ with

$$e_y = \frac{1}{\pi\sqrt{(W_{a1}/2)^2 - y^2}} \cos\left(\frac{\pi x}{L_{a1}}\right), \tag{2}$$

n_f can be calculated efficiently[6][7] using the spectral-domain immittance approach and the finite Fourier transform[11]. The value of n_p can be evaluated in a similar manner.

2. Evaluation of the Aperture Admittance

The coupled power to the aperture from the feed line is transferred to the lower half space as well as the cavity in the thick ground plane. The complex power flow into the lower half space can be

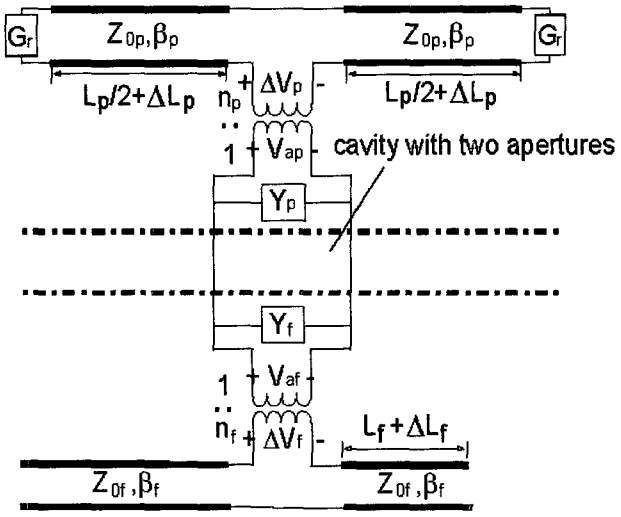

그림 2. 개구면 결합 공진기 급전 마이크로스트립 패치 안테나의 등가회로 초안

Fig. 2. Draft equivalent circuit of aperture-coupled cavity-fed microstrip patch antenna.

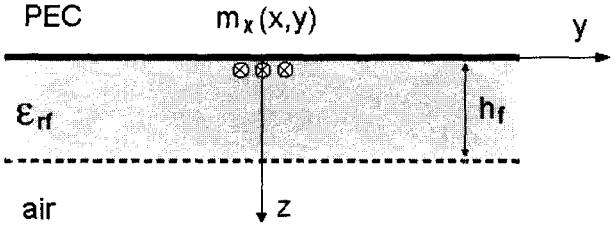

그림 3. 자류에 의해 급전되는 접지면 아래쪽 유전체의 구조

Fig. 3. Structure of the lower half space with a dielectric substrate excited by magnetic current.

computed from the equivalent magnetic current source $\bar{m}$ on the perfect electric conductor(PEC) as shown in Fig. 3, where $\bar{m}$ is determined by the equivalence theorem[9] as $\bar{m} = \bar{e}_a \times \hat{n}$. The resulting $\bar{m}$ is given as $\bar{m} = \hat{x} m_x$, where the expression for m_x is the same as that for e_y.

Because the maximum voltage value across the aperture becomes $1V$ from the assumed aperture electric field distribution, the admittance looking into the lower half space from the aperture 1, $Y_f(= G_f + jB_f)$, is expressed by applying the complex power concept[9] as

$$Y_f = -\iint_{S_a} m_x^* h_x\, dS, \tag{3}$$

where m_x^* denotes the complex conjugate of m_x, and m_x^* is the x-component of the magnetic field at the aperture 1 induced by the magnetic current m_x. If the Fourier transform is chosen as

$$\tilde{\Phi}(k_x, k_y) = \int_{-\infty}^{\infty}\int_{-\infty}^{\infty} \Phi(x, y)\, e^{j(k_x x + k_y y}\, dx dy, \qquad (4)$$

Y_f is expressed by applying Parceval's theorem[11] as

$$Y_f = \frac{-1}{4\pi^2}\int_{-\infty}^{\infty}\int_{-\infty}^{\infty} \tilde{G}_{xx}^{HM}\, \tilde{M}_x^{\,2}\, dk_x dk_y, \qquad (5)$$

where $\tilde{G}_{xx}^{HM}$, the spectral-domain Green's function of h_x due to m_x, is given with the spectral-domain immittance approach[11] as

$$\tilde{G}_{xx}^{HM} = \frac{-k_x^2}{k_x^2 + k_y^2} Y_{TE} + \frac{-k_y^2}{k_x^2 + k_y^2} Y_{TM}, \qquad (6)$$

where Y_{TE} and Y_{TM} are the input wave admittances for the TE_z and TM_z modes, respectively. In equation (5), $\tilde{M}_x$, the Fourier transform of m_x, is given as

$$\tilde{M}_x = \frac{2\pi}{L_{a1}} \frac{cos(k_x L_{a1}/2)}{(\pi/L_{a1})^2 k_x^2} \cdot J_0\left(\frac{W_{a1}}{2} k_y\right), \qquad (7)$$

where $J_0(\cdot)$ denotes the zero-order Bessel function of the first kind.

With the coordinate transformations ($k_x = k_\rho cos\phi$ and $k_x = k_\rho sin\phi$) and the symmetry property of $\tilde{G}_{xx}^{HM}$ and $\tilde{M}^2$, Y_f can be reformed as

$$Y_f = \frac{-1}{\pi^2}\int_0^{\pi/2}\int_0^{\infty} \tilde{G}_{xx}^{HM}\, \tilde{M}_x^{\,2} k_\rho\, dk_\rho d\phi, \qquad (8)$$

where the integrand is known to have a singular point for $k_0 < k_\rho < k_0\sqrt{\epsilon_{rf}}$ due to the surface wave pole of the TM_z mode, and have very oscillatory and slow convergence characteristics as k_ρ increases. To overcome these difficulties in the calculation of, the singularity extraction and the asymptotic extraction techniques[12][13] are invoked, and the integral can be numerically evaluated without difficulty.

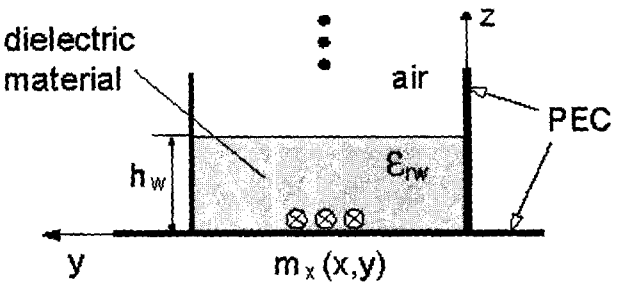

그림 4. 자류에 의해 급전되는 도파관 구조
Fig. 4. Structure of the waveguide excited by a magnetic current.

Detailed evaluations are described in Appendix. $Y_p(= G_p + jB_p)$ can be calculated similarly.

3. Modeling of a Cavity with Two Apertures

The rectangular cavity with two apertures in the antenna consists of two aperture-to-waveguide sections in a back-to-back configuration. First, modeling of the section of the aperture-to-waveguide in the feed side, shown in Fig. 4, is considered. $Y_w(= G_w + jB_w)$, the input admittance looking into the waveguide from the aperture 1, has the same expression as that of Y_f in equation (3) with h_x replaced by h_{wx}, the x-component of the magnetic field in the waveguide induced by m_x.

TE_x formulation has been efficiently used for the analysis of waveguide step discontinuity problem[9]. But this method cannot be applied to the waveguide structure filled with multi-dielectric layers in the longitudinal direction. So, the spectral-domain immittance approach, which has been widely used for the analysis of multi-layer planar microwave circuits, is chosen to find Green's functions efficiently for a metallic waveguide structure considered in this paper.

Because the region of the problem is confined by a metallic wall, the Fourier series representation is adopted for the expression of the electromagnetic field instead of the Fourier transform. Considering the field behavior of h_{wx} in the waveguide, the Fourier

series is chosen as

$$\Phi(x,y)=\sum_{m,n}\Phi_{mn}sink_{xm}xcosk_{yn}y, \quad (9)$$

where $k_{xm}=m\pi/a(m=1,2,\cdots)$, $k_{yn}=n\pi/b(n=0,1,2,\cdots)$, and Φ_{mn} is the Fourier coefficient of $\Phi(x,y)$.

With this definition and applying Parceval's theorem, Y_w is expressed as

$$Y_w=-\sum_{m=1}^{\infty}\sum_{n=0}^{\infty}\frac{ab}{2\epsilon_n}(\tilde{G}_{xx}^{HM})_{mn}(\tilde{M}_x)_{mn}^{2}, \quad (10)$$

where $\epsilon_n=1$ for $n=0$, $\epsilon_n=2$ for $n\neq 0$. $(\tilde{G}_{xx}^{HM})_{mn}$, the mn-th mode spectral-domain Green's function of h_{wx} due to m_x, can be efficiently found with the help of the spectral-domain immittance approach, and has the same expression as that of $\tilde{G}_{xx}^{HM}$ in equation (6) with all the related parameters replaced by the modified parameters with k_x and k_y substituted by k_{xm} and k_{yn}, respectively. In equation (10), $(\tilde{M}_x)_{mn}$, the Fourier coefficient of m_x, is given as

$$(\tilde{M}_x)_{mn}=\frac{2\epsilon_n}{ab}\frac{2\pi}{L_{a1}}\frac{\cos(k_{xm}L_{a1}/2)\sin(k_{xm}a/2)}{(\pi/L_{a1})^2-k_{xm}^2}\cdot J_0\left(\frac{W_{a1}}{2}k_{yn}\right)\cos\left(\frac{k_{yn}b}{2}\right). \quad (11)$$

With some algebraic manipulations, Y_w is reduced to

$$Y_w=\sum_{m=1}^{\infty}\sum_{n=0}^{\infty}\{(n_{mn}^{TE})^2Y_{mn}^{TE}+(n_{mn}^{TM})^2Y_{mn}^{TM}, \quad (12)$$

where $(n_{mn}^{TE})^2$ is given as

$$(n_{mn}^{TE})^2=\frac{ab}{2\epsilon_n}\frac{k_{xm}^2}{k_{xm}^2+k_{yn}^2}(\tilde{M}_x)_{mn}^{2}, \quad (13)$$

and the expression of $(n_{mn}^{TM})^2$ is the same as that of $(n_{mn}^{TE})^2$ with k_{xm} and k_{yn} interchanged. Because n_{mn}^{TE} and n_{mn}^{TM} can be regarded as the turns ratios of the ideal transformers between the corresponding waveguide mode voltages and the aperture voltage, the aperture-to-waveguide structure can be modeled as the equivalent circuit shown in Fig. 5, where characteristics of each mode of a waveguide is reflected by the corresponding equivalent transmi -ssion line. The opposite section can be modeled similarly, and the equivalent circuit of a cavity with two apertures is obtained as shown in Fig. 6.

4. Equivalent Circuit and Design Procedure

The characteristics of the circuit with transformers and transmission lines of mn-th TE_z mode in the dotted box shown in Fig. 6 can be analyzed using the ABCD matrix formulation, where the resulting ABCD matrix is equal to the successive multiplication

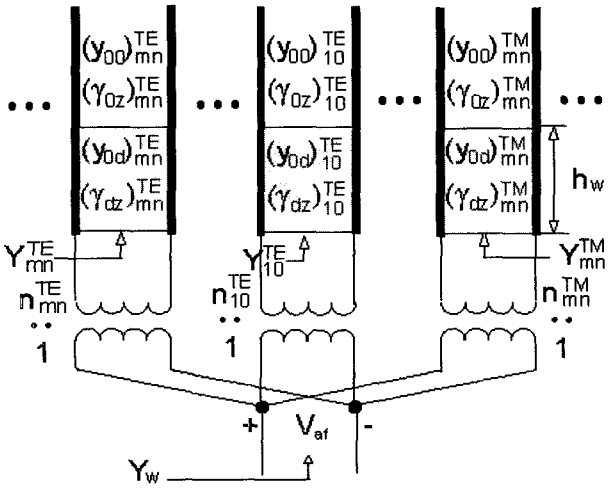

그림 5. 개구면 급전 도파관의 등가회로
Fig. 5. Equivalent circuit of aperture-to-waveguide section.

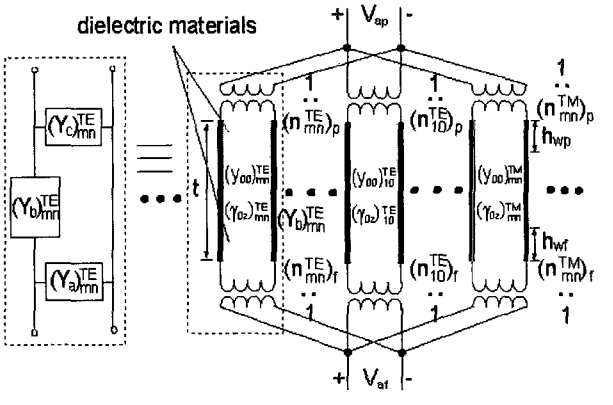

그림 6. 두 개의 개구면을 포함한 공진기의 등가회로
Fig. 6. Equivalent circuit of a cavity with two aperture.

multiplication of the individual ABCD matrices[14]. From the obtained ABCD matrix, the admittance parameters of the equivalent π-network shown in Fig. 6 are obtained by the conversion relations between the two-port network parameters[14]. App -ing this procedure to the other transmission line sections, the corresponding parallel-connected π -networks are obtained, and all of these π-networks are simplified to one π-network as shown in Fig. 7. The characteristics of the overall antenna circuit can therefore be calculated using the well-known micro -ve network theory[14].

For impedance matching, $Z_{in} = 50\,\Omega$ should be met, where $Z_{in} = R_1 + j(X_1 + X_f)$. At first, structure parameters should be determined to satisfy the relation of $R_1 = 50\,\Omega$ by the parameter sweep. Next, the remaining imaginary value X_1 can be cancelled out under the condition of $X_f = -X_1$ by adjusting the stub length.

III. RESULT AND DISCUSSION

To check the validity of the theory, the structure had described in the published paper[5] was considered. The rectangular cavity is filled with a dielectric material with $\epsilon_{rw} = 10.2$. The other parameters of the waveguide structure are $L_p = 32.50\,mm$, $W_p = 27.50\,mm$, $h_p = 1.60\,mm$, $\epsilon_{rp} = 2.20$, $L_{a1} = 12.00\,mm$, $W_{a1} = 1.27\,mm$, $L_{a2} = 20.00\,mm$, $W_{a2} = 1.27\,mm$, $a = 37.00\,mm$, $b = 1.27\,mm$, $t = 14.80\,mm$, $W_f = 2.47\,mm$, $h_f = 0.79\,mm$, $\epsilon_{rf} = 2.20$, and $L_f = 17.40\,mm$. Computed Y_f, Y_{ap}, n_f, and n_p are shown in Figs. 8 and 9, and the calculated susceptances $B_a(Y_a = jB_a)$, $B_b(Y_b = jB_b)$, and $B_c(Y_c = jB_c)$ are shown in Fig. 10.

From these computed circuit parameters, the input impedance was computed. The result is shown in Fig. 11 along with the published measured and calculated data. Good agreements show the validity and accuracy of the present equivalent circuit modeling.

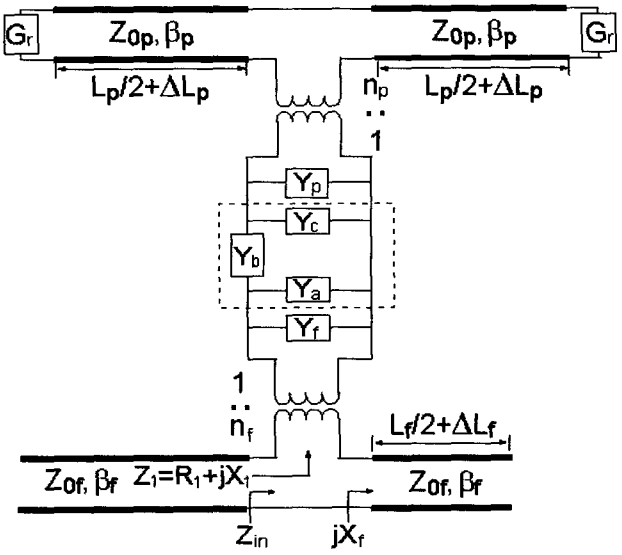

그림 7. 개구면 결합 공진기 급전 마이크로스트립 패치 안테나의 간략화한 등가회로

Fig. 7. Simplified equivalent circuit of aperture-coupled cavity-fed microstrip patch antenna.

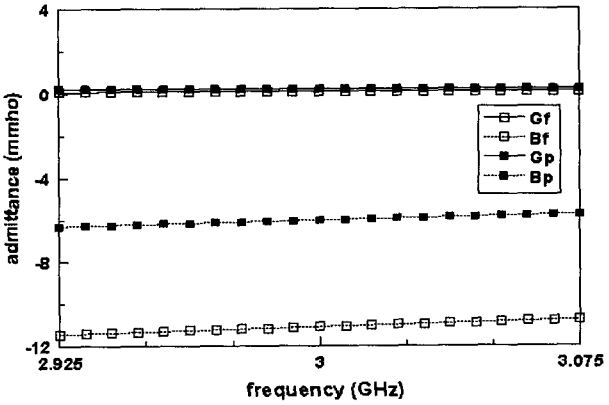

그림 8. 계산된 개구면 어드미턴스

Fig. 8. Computed aperture admittances.

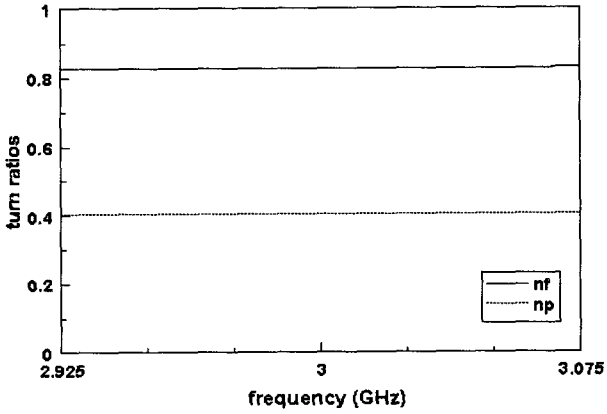

그림 9. 이상적 트랜스의 권선비(n_f, n_p)

Fig. 9. Computed turn ratios.

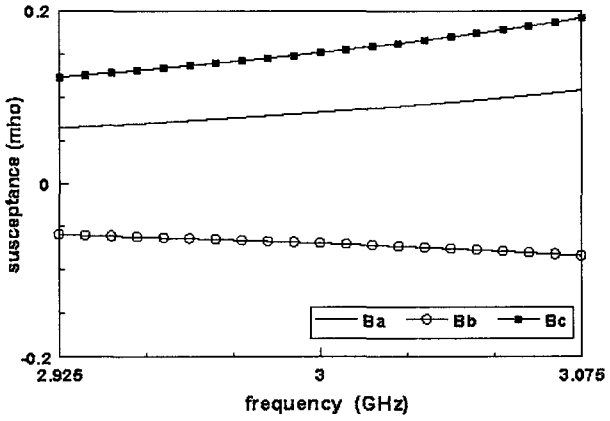

그림 10. 등가 π모델의 계산된 susceptance값
Fig. 10. Computed susceptances of the equivalent π -network.

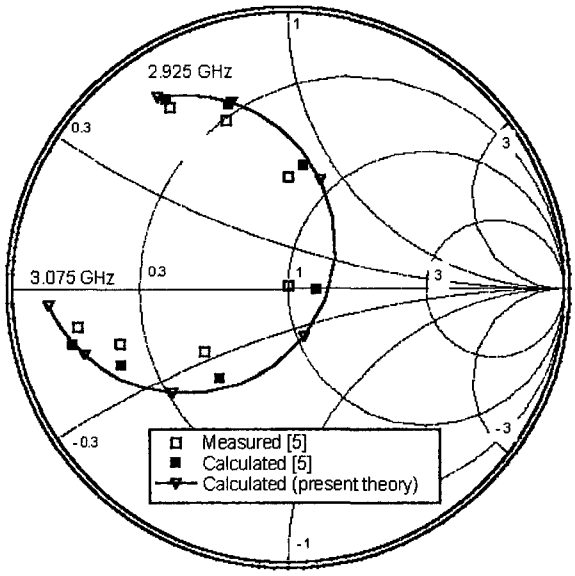

그림 11. 입력 임피던스의 계산 결과
Fig. 11. Input impedance of the antenna.

IV. CONCLUSIONS

A general theory for the analysis of an aperture -coupled cavity-fed microstrip patch antenna was presented for developing an efficient and accurate equivalent circuit model. The equivalent circuit consists of ideal transformers, admittance elements, and transmission lines reflecting the corresponding modes of a waveguide. It was simplified using the ABCD matrix formulation and parameter conversion. The computed results from this theory was compared with the measured and the published calculated data, and good agreements fully indicated the validity of the proposed modeling.

APPENDIX

Because $f(k_\rho, \phi)$ in equation (8) has a singularity in the region of $k_0 < k_\rho < k_0\sqrt{\varepsilon_f}$, Y_f can be calculated efficiently after domain decomposition as

$$Y_f = \frac{-1}{\pi^2}[I_1 + I_2 + I_3], \tag{14}$$

with

$$I_1 = \int_0^{\pi/2}\int_0^{k_0} f(k_\rho, \phi)\, dk_\rho d\phi, \tag{15}$$

$$I_2 = \int_0^{\pi/2}\int_{k_0}^{k_0\sqrt{\epsilon_f}} f(k_\rho, \phi)\, dk_\rho d\phi, \tag{16}$$

$$I_3 = \int_0^{\pi/2}\int_{k_0\sqrt{\epsilon_f}}^{\infty} f(k_\rho, \phi)\, dk_\rho d\phi. \tag{17}$$

A.1.. Calculation of I_1

$f(k_\rho, \phi)$ becomes steep near $k_\rho = k_0$. This problem can be avoided by applying a change of variables of $k_\rho = k_0 \sin\theta$. Now I_1 is reformed as

$$I_1 = \int_0^{\pi/2}\int_0^{\pi/2} f(k_\rho, \phi) k_0 \cos\theta\, d\theta d\phi, \tag{18}$$

and it can be calculated easily by direct integration.

A.2.. Calculation of I_2

In this case, $f(k_\rho, \phi)$ has a singularity due to the pole of the TM_z surface wave mode. The pole location can be found using root-seeking algorithms, such as the Newton-Raphson method or the bisection method[15]. After finding the pole location $k_{\rho 0}$, I_2 can be calculated without difficulty by applying the singularity extraction technique[12] as explained below. In equation (16), $f(k_\rho, \phi)$ can be expressed as

$$f(k_\rho,\phi)=\frac{g(k_\rho,\phi)}{k_\rho-k_{\rho 0}}, \tag{19}$$

with

$$g(k_\rho,\phi)=(k_\rho-k_{\rho 0})f(k_\rho,\phi). \tag{20}$$

Because $g(k_\rho,\phi)$ becomes non-singular at $k_\rho=k_{\rho 0}$ I_2 can be recast as

$$\begin{aligned} I_2 &= \int_0^{\pi/2}\int_{k_0}^{k_0\sqrt{\epsilon_f}}\frac{g(k_\rho,\phi)}{k_\rho-k_{\rho 0}}\,dk_\rho\,d\phi, \\ &= \int_0^{\pi/2}\left[\int_{k_0}^{k_0\sqrt{\epsilon_f}}\left\{\frac{g(k_\rho,\phi)-g(k_{\rho 0},\phi)}{k_\rho-k_{\rho 0}}+\frac{g(k_{\rho 0},\phi)}{k_\rho-k_{\rho 0}}\right\}dk_\rho\right]d\phi, \\ &= \int_0^{\pi/2}\int_{k_0}^{k_0\sqrt{\epsilon_f}}\frac{g(k_\rho,\phi)-g(k_{\rho 0},\phi)}{k_\rho-k_{\rho 0}}\,dk_\rho\,d\phi \\ &\quad+ln\left(\frac{k_0\sqrt{\epsilon_f}-k_{\rho 0}}{k_{\rho 0}-k_0}\right)\int_0^{\pi/2}g(k_{\rho 0},\phi)\,d\phi \\ &\quad-j\pi\int_0^{\pi/2}g(k_{\rho 0},\phi), \end{aligned} \tag{21}$$

and can be calculated without difficulty.

A.3. Calculation of I_3

I_3 is an infinite integral with the highly oscillating and slowly converging integrand as k_ρ increases. For efficient calculation of this type of integral, the asymptotic extraction technique[13] usually can be used. Define $f_a(k_\rho,\phi)$, the asymptotic term of $f(k_\rho,\phi)$, as

$$\begin{aligned} &f_a(k_\rho,\phi)\triangleq \\ &\lim_{\rho\to\infty}f(k_\rho,\phi)=\tilde{G}_{xxa}^{HM}(k_\rho,\phi)\,\tilde{M}(k_\rho,\phi)^2k_\rho, \end{aligned} \tag{22}$$

where $\tilde{G}_{xxa}^{HM}(k_\rho,\phi)$, the asymptotic Green's function of $\tilde{G}_{xx}^{HM}(k_\rho,\phi)$, is given by

$$\tilde{G}_{xxa}^{HM}(k_\rho,\phi)=\lim_{k_\rho\to\infty}\tilde{G}_{xx}^{HM}(k_\rho,\phi). \tag{23}$$

In the above equation, $k_\rho\to\infty$ implies that all the half space is filled with a dielectric material with a dielectric constant of ε_{rf}. Therefore $\tilde{G}_{xxa}^{HM}(k_\rho,\phi)$ becomes

$$\begin{aligned} \tilde{G}_{xxa}^{HM}(k_\rho,\phi) &= -y_{0d}^{TE}cos^2\phi-y_{0d}^{TM}sin^2\phi \\ &= \frac{1}{jw\mu_0}\frac{k_0^2\epsilon_{rf}-k_x^2}{\gamma_{od}}. \end{aligned} \tag{24}$$

Now I_3 can be expressed as

$$I_3=I_{3a}+I_{3d}, \tag{25}$$

with

$$I_{3a}=\int_0^{\pi/2}\int_{k_0\sqrt{\epsilon_{rf}}}^{\infty}f_a(k_\rho,\phi)\,dk_\rho\,d\phi, \tag{26}$$

$$I_{3d}=\int_0^{\pi/2}\int_{k_0\sqrt{\epsilon_{rf}}}^{\infty}f_d(k_\rho,\phi)\,dk_\rho\,d\phi, \tag{27}$$

where $f_d(k_\rho,\phi)(=f(k_\rho,\phi)-f_a(k_\rho,\phi))$ is the integrand with an asymptotic term extracted.

From equation (26), I_{3a} is given as

$$\begin{aligned} I_{3a} &= \int_0^{\pi/2}\int_{k_0\sqrt{\epsilon_{rf}}}^{\infty}\tilde{G}_{xxa}^{HM}(k_\rho,\phi)\,\tilde{M}(k_\rho,\phi)^2k_\rho\,dk_\rho\,d\phi, \\ &= \iint_{k_x^2+k_y^2\geq k_0^2\epsilon_{rf}}\frac{1}{jw\mu_0}\frac{k_0^2\epsilon_{rf}-k_x^2}{\gamma_{0d}} \\ &\quad\times\tilde{M}(k_\rho,\phi)^2\,dk_x\,dk_y \end{aligned} \tag{28}$$

Because $\tilde{M}(k_x,k_y)$ can be separated into two functions of k_x and k_y, respectively, as

$$\tilde{M}(k_x,k_y)=X(k_x)\cdot Y(k_y), \tag{29}$$

with

$$\begin{aligned} X(k_x)&=\frac{2\pi}{L_{a1}}\frac{\cos(k_xL_{a1}/2)}{(\pi/L_{a1})^2-k_x^2}, \\ Y(k_y)&=\frac{\sin(k_yW_{a1}/2)}{k_yW_{a1}/2}, \end{aligned} \tag{30}$$

I_{3a} is expressed as

$$I_{3a} = I_{3a1} + I_{3a2}, \tag{31}$$

with

$$I_{3a1} = \frac{1}{j\omega\mu_0}\int_0^{k_0\sqrt{\epsilon_{rf}}}(k_0^2\epsilon_{rf} - k_x^2)X^2(k_x) \cdot \left(\int_{\sqrt{k_0^2\epsilon_{rf}-k_x^2}}^{\infty}\frac{Y^2(k_y)}{\gamma_{od}}dk_y\right)dk_x, \tag{32}$$

$$I_{3a2} = \frac{1}{j\omega\mu_0}\int_{k_0\sqrt{\epsilon_{rf}}}^{\infty}(k_0^2\epsilon_{rf} - k_x^2)X^2(k_x) \cdot \left(\int_0^{\infty}\frac{Y^2(k_y)}{\gamma_{od}}dk_y\right)dk_x. \tag{33}$$

Using the following relations[16][17]:

$$\int_{\sqrt{k_0^2\epsilon_{rf}-k_x^2}}^{\infty}\frac{Y^2(k_y)}{\gamma_{od}}dk_y = \frac{3}{2} - \gamma - ln\ \frac{W_{a1}}{2}\sqrt{k_0^2\epsilon_{rf}-k_x^2}, \tag{34}$$

$$\int_0^{\infty}\frac{Y^2(k_y)}{\gamma_{od}}dk_y = \frac{3}{2} - \gamma - ln\ \frac{W_{a1}}{2}\sqrt{k_x^2-k_0^2\epsilon_{rf}}, \tag{35}$$

with Euler's constant $\gamma \cong 0.5772$, I_{3a} becomes an one-dimensional integral as

$$I_{3a} = \frac{1}{j\omega\mu_0}\int_0^{\infty}(k_0^2\epsilon_{rf} - k_x^2)X^2(k_x) \cdot \left(\frac{3}{2} - \gamma - ln\ \frac{W_{a1}}{2}\sqrt{k_x^2 - k_0^2\epsilon_{rf}}\right)dk_x, \tag{36}$$

and can be easily calculated numerically. Now, $f_d = (k_\rho, \phi)$ becomes very convergent, and the two-dimensional integral I_{3d} can therefore be integrated numerically without difficulty.

References

[1] D. M. Pozar, "Microstrip antenna aperture-coupled to a microstripline," *Electron. Lett.*, vol. 21, pp. 49-50, Jan. 1985.

[2] G. Splitt and M. Davidovitz, "Guidelines for design of electromagnetically coupled microstrip patch antennas on two-layer substrates," *IEEE Trans. Antennas Propagat.*, vol. 38, no. 7, pp 1136-1990, Jul. 1990.

[3] M. Davidovitz, R. A. Sainati, and S. J. Fraasch, "A non-contact interconnection through an electrically thick ground plate common to two microstrip lines," *IEEE Trans. Microwave Theory Tech.*, vol. 43, no. 4, pp. 753-759, Apr. 1995.

[4] P. R. Haddad and D. M. Pozar, "Characterization of aperture-coupled microstrip patch antenna with thick ground plane," *Electron. Lett.*, vol. 30, no. 14, pp. 1106-1107, Jul. 1994.

[5] P. R. Haddad and D. M. Pozar, "Analysis of two aperture-coupled cavity-backed antennas," *IEEE Trans. Antennas Propagat.*, vol. AP-45, no. 12, pp. 1717-1726, Dec. 1997.

[6] J. P. Kim and W. S. Park, "An improved network modeling of slot-coupled microstrip lines," *IEEE Trans. Microwave Theory Tech.*, vol. MTT-46, no. 10, pp. 1484-1491, Oct. 1998.

[7] J. P. Kim and W. S. Park, "Analysis and network modeling of an aperture-coupled micro -strip patch antenna," *IEEE Trans. Antennas Propagat.*, vol. AP-49, no. 6, pp. 849-854, Jun. 2001.

[8] R. Garg, P. Bhartia, I. Bahl, and A. Ittipiboon, *Microstrip Antenna Design Handbook*, Artech House, 2001.

[9] R. F. Harrington, *Time Harmonic Electromagnetic Fields*, IEEE Press, 2001.

[10] D. M. Pozar, "A reciprocity method of analysis for printed slot and slot-coupled microstrip antennas," *IEEE Trans. Antennas and Propagat.*, vol. AP-34, no. 12, pp. 1439-1446, Dec. 1986.

[11] T. Itoh, "Spectral domain immittance approach for dispersion characteristics of generalized printed transmission lines," *IEEE Trans. Micro -wave Theory Tech.*, vol. MTT-28, no. 7, pp. 733-736, Jul. 1980.

[12] A. K. Bhattacharyya, *Electromagnetic Fields in Multilayered Structures*, Artech House, 1994.

[13] H. Y. Yang, *Frequency Dependent Modeling of Passive Integrated Circuit Components*, Ph.D. thesis, University of California, Los Angeles, 1988.

[14] D. M. Pozar, *Microwave Engineering.*, 2nd ed., John Wiley & Sons, 1998.

[15] R. L. Burden and J. D. Faires, *Numerical Analysis*, 7th ed., Brooks Cole, 2000.

[16] D. R. Rhodes, "On a fundamental principle in the theory of planar antennas," *Proc. IEEE,*

vol. 52, pp 1013-1021, Sep. 1964.
[17] N. B. Das and M. Sinha, "The admittance characteristics of longitudinal shunt slots in the broad face of rectangular waveguide," *Journal of Inst. Electron. Telecom*, vol. 21, pp. 32-37, Jan. 1975.

저 자 소 개

신 종 우(학생회원)
2003년 2월 중앙대학교 전자전기공학부 (공학사)
2003년 3월~현재 중앙대학교 전자전기공학부 석사과정
<주관심분야: 안테나 설계 및 수동 소자>

김 정 필(정회원)
1988년 2월 서울대학교 전자공학과(공학사).
1990년 2월 포항공과대학교 전자전기공학과(공학석사).
1998년 2월 포항공과대학교 전자전기공학과(공학박사).
1990년 1월~2001년 2월 LG 이노텍(주) 연구소 책임연구원
2001년 3월~현재 중앙대학교 전자전기공학부 조교수
<주관심분야: 마이크로파 회로설계, 마이크로스트립 안테나 설계, 무선통신용 송수신 시스템 및 부품 설계>